PCCP

Accepted Manuscript

ROYAL SOCIETY OF CHEMISTRY

www.rsc.org/pccp

Molecular material based on electropolymerized cobalt macrocycle for electrocatalytic hydrogen evolution

Stéphane Rioual,[1] Benoit Lescop,[1] François Quentel,[2] Frederic Gloaguen[2,*]

[1]LMB EA 4522, [2]CEMCA UMR 6521, CNRS, Université de Bretagne Occidentale, Brest, France

E-mail: fgloague@univ-brest.fr (FG)

Abstract

Electrocatalytic material for the H_2 evolution reaction (HER) in acidic aqueous solution has been prepared by electropolymerization of Co(II) dibenzotetraaza[14] annulene (CoTAA). Chemical analysis by X-ray photoelectron spectroscopy (XPS) confirms that the structural integrity of the [Co^{II}–N_4] motif is preserved in the poly-CoTAA film. In acetate buffer solution at pH 4.6, an overpotential $\eta = -0.57$ V is required to attain a catalytic current density $-i_k = 1$ mA cm^{-2}_{geom}. The faradaic efficiency of poly-CoTAA for the HER is 90% over a period of one hour of electrolysis, but there is a decrease of the apparent concentration of Co sites after prolonged H_2 production, we ascribe to partial demetallation of the poly-CoTAA film at negative potentials.

Introduction

Despite long history, H_2 production from electrochemical water reduction is still a matter of considerable attention.[1, 2] Besides, this energy conversion process could help solving the problem of energy transition.[3, 4] Although platinum is a very efficient catalyst for the H_2 evolution reaction (HER),[5, 6] recent efforts are devoted to the development of cheaper and more abundant catalytic materials.[7] In this context, inorganic materials have emerged as potential substitutes of platinum, especially those based on transition metal sulfides.[8-12] On the other hand, molecular catalysts employing transition metal complexes offer the prospect of rational design by judicious choice of the

metal center and systematic modification of the steric and electronic properties of the ligands.[13-17] Numerous first row transition metal complexes have been shown to catalyze the HER in solution.[18-21] Among them, cobalt complexes have been extensively studied thanks to versatile redox chemistry.[4, 22-25] Furthermore, electrode materials capable of evolving H_2 from water have been prepared by immobilization of various types of cobalt complexes.[17, 26-31] However, retention of structural integrity and catalytic activity upon immobilization remains challenging. The stability of molecular catalysts under reducing and acidic conditions has also been questioned.[32-35]

The ligand dibenzotetraaza[14] annulene (TAA) and its tetramethyl derivative(TMTAA) have been studied as mimics of porphyrin rings.[36, 37]. Because of a short metal–nitrogen bond, transition metal complexes of TAA are comparatively resistant to demetallation. For example, CoTAA has been employed to electrocatalyze the oxygen reduction in concentrated sulfuric acid solution.[38] Furthermore, Bereman and coworkers have reported that NiTMTAA polymerizes upon electrochemical oxidation,[39], giving a poly-NiTMTAA film that is electrocatalytically active for CO_2 reduction.[40] Pt, Pd, and Cu complexes of TMTAA have also been polymerized by electrochemical oxidation.[41-43]. L'Her and coworkers have studied the electropolymerization of CoTMTAA and CoTAA, showing that a poly-CoTAA film can be grown on various electrode materials by continuous potential scanning in a CoTAA/benzonitrile solution.[44]

In previous work, we have shown that a poly-CoTAA is catalytically active and stable for oxygen reduction under fuel cell operating conditions.[45] Herein we report the further investigation of poly-CoTAA as a molecular material for electrocatalyzis of the HER in acidic aqueous solution.

Experimental details

CoTAA (Scheme 1) was synthesized according to published procedures,[45] and further characterized by UV-visible spectrum (Fig. S1 of ESI). All the solutions were prepared from analytical-grade salts and distilled benzonitrile (PhCN), HPLC-grade acetonitrile (MeCN), or deionized water (Millipore Milli-

Q). The solutions were purged with N_2 (Alphagaz 1). The pH of aqueous solutions was controlled with a glass electrode connected to a pH-meter (Hanna HI 2221).

The electrochemical measurements were carried in a three-electrode glass cell connected to a potentiostat (Autolab PGSTAT12 with SCANGEN option). The working electrodes were either a gold coated glass slides of about 1 cm^2 in surface area or a glassy carbon (GC) tips of 0.071 cm^2 in surface area mounted on a rotating disk electrode (RDE, EDI101 Radiometer Analytical). The Au coated glass slides were prepared by radio frequency sputter deposition. A thin chromium layer of ca. 5 nm was deposited on the glass slide prior to deposition of a gold layer of ca. 100 nm, allowing good adhesion and avoiding delamination of the gold layer. The Au coated glass slides were cleaned with acetone, while the GC tips were polished with alumina powder (Presi, 0.3 µm) and rinsed with water and acetone. Ferrocene (Fc) was used as an internal standard for the potential scale in organic solvent. In aqueous solution, the reference electrode was a saturated calomel electrode (SCE, Radiometer Analytical) and the counter-electrode a high purity graphite rod (Le Carbone Lorraine).

Electrolymerization was carried out by 30 voltammetric cycles at 0.1 V s^{-1} in a freshly prepared solution of 0.1 M Bu_4NPF_6/PhCN saturated with CoTAA, i.e. about 2 mM of CoTAA. The apparent concentration of Co sites was obtained by demetallation of the poly- CoTAA film in aqua regia (HCl/HNO_3 3/1 in vol.), and analysis of the resulting Co solution by cathodic stripping voltammetry using a method adapted from the literature.[46] Briefly, the poly-CoTAA modified GC electrode was immerged in aqua regia (0.5 mL) and placed in an ultrasound bath for 30 min. Following that, a stock solution (20 mL) was prepared by addition of ammonia buffer (0.4 M), nitrite (0.1 M) and nioxime (50 µM). After dilution of the stock solution by a factor of 2,000 to 4,000, the Co concentration was determined by cathodic stripping voltammetry (E_{dep} = –0.7 V vs. SCE for 100 s) using the method of standard addition.

The HER kinetics was measured at poly-CoTAA modified GC RDEs at a scan rate of 5 mV s^{-1} and rotation rates in the range 100–500 rpm in N_2-purged 0.1 M NaCl buffered solutions at room temperature of ca. 17 ±1 °C. A Luggin capillary was used to limit the effect of ohmic drop on the

voltammograms. For prolonged H_2 evolution measurements, the counter electrode was separated from the working electrode compartment by a glass frit. A Pt RDE was used to calibrate the catalytic performances of the poly-CoTAA film. Before recording the catalysis of the HER at the Pt RDE, the Pt surface was cleaned by 10 scans at 0.1 V s^{-1} between –0.6 to +1.0 V vs. SCE in acetate buffer solution. From the value of half-wave potential of the voltammogram recorded at a Pt RDE, the reversible potential of the HER was estimated to be $E^0_{H+/H2}$ = –0.52 V vs. SCE at pH 4.6. Conversion to the SHE scale can be achieved by adding 0.244 V to the potential values experimentally measured vs. the SCE. Correction of the voltammograms for mass-transfer limitation was performed according to the following equation: $i_k = (i \times i_L)(i_L - i)^{-1}$, in which i_L is the limiting current density at a rotation rate ω. This procedure was used to calculate Tafel plots; i.e. η vs. $\log(-i_k)$ plots, where $\eta = E - E^0_{H+/H2}$ is the overpotential and i_k the current density under pure activation control.

XPS analysis of the CoTAA film electropolymerized on an Au-coated glass slide electrode was carried out using the setup described elsewhere.[47] Co(II)-tetraphenylporphyrin (CoTPP, Sigma-Aldrich) glued on a glass slide by an adhesive tape was used as a [Co^{II}–N_4] reference compound. The XPS signals were scaled considering that the energy of the C–C bonds is 284.8 eV. Fitting procedures were applied to derive the amplitude of the different peaks observed on the spectra.

Results and discussion

Electropolymerization of CoTAA

The voltammograms recorded at an Au-coated glass slide electrode in a solution of CoTAA in Bu_4NPF_6/PhCN display on the first and second scans the peaks associated with the electrochemical reactivity of free-diffusing CoTAA (Fig. 1 and Fig. S2 of ESI). The redox event at $E_{1/2}$ = –0.28 V vs. $Fc^{+/0}$ is metal centered and assigned to the Co(III)/Co(II) couple, while that at $E_{1/2}$ = 0.42 V vs. $Fc^{+/0}$ is ligand centered.[44, 48] It has been previously established that electropolymerization of CoTAA can be achieved when the electrode is set at a potential value more positive than that of the second

oxidation of the ligand,[44, 45] occurring here at $E_{1/2}$ = +0.74 V vs. $Fc^{+/0}$. The voltammogram recorded after 30 scans confirms accumulation of poly-CoTAA on the electrode surface (Fig. 1). The capacitance of the electrode has distinctly increased along with the charge density associated with the Co(III)/Co(II) redox process. But, the evolution of the CV shape between the first and the 30st cycles is also indicative of a slow growth of the poly-CoTAA film. This observation is apparently contradictory with that of a fast polymerization rate achieved under very similar electrochemical conditions with Ni, Pd and Pt complexes of TMTAA.[41]. Previous studies have established that the first step of the electropolymerization process is the one-electron oxidation of the ligand to give a dimer, which then polymerizes upon further oxidation.[39] However, in contrast with what has been observed for Ni, Pd and Pt complexes of TMTAA, the first ligand oxidation of CoTAA is chemically reversible on the voltammetric timescale (Fig. 1), indicating a slow dimerization rate, and explaining thus the slow electropolymerization rate. Even slower rate has been reported for CoTMTAA,[44] suggesting that the oxidation processes of the TAA and TMTAA ligands, and hence the electropolymerization process, is greatly influenced by the nature of the coordinated metal ion.[36]

To determine electrocatalytic parameters from kinetic measurements at a RDE coated with an electroactive film, one has to ensure that mass transfer and electronic and ionic conductions within the film will not be rate limiting.[49] Here, GC RDEs are coated with a thin poly-CoTAA film formed upon 30 potential scans between –0.8 V and 0.8 V vs. $Fc^{+/0}$ in a solution of CoTAA in Bu_4NPF_6/PhCN (Fig. S3 of ESI). However, for such thin poly-CoTAA film, the apparent surface concentration of Co sites is difficult to estimate from integration of the voltammetric peaks associated with the Co(III)/Co(II) couple (Fig. S4 of ESI).[28] Instead, the amount of Co is determined by cathodic stripping voltammetry after demetallation of the poly-CoTAA film in aqua regia (see Experimental details). Six independent analyses of poly-CoTAA films formed upon 30 scans on a GC electrode give an average surface concentration of 1.44 ±0.40 $\times$ 10^{-8} (mol Co) cm^{-2}, indicating that the electropolymerization conditions chosen here result in poly-CoTAA films with a reproducible thickness. The apparent surface concentration of Co sites within the poly-CoTAA film is comparable

with that achieved by grafting a Co diimine-dioxime complex at the surface of carbon nanotubes.[28], but two orders of magnitude lower than that reported for electrodes modified by Co dithiolene in metal-organic framework (Table 1).[31]

XPS analysis of poly-CoTAA

The survey spectrum of the poly-CoTAA film formed on an Au-coated glass slide electrode upon 30 scans between –0.8 V and 1.1 V vs $Fc^{+/0}$ in a solution of CoTAA in Bu_4NPF_6/PhCN indicates the presence of Co, C, N and O elements (Fig. S5 of ESI). The gold substrate is not observed due a thickness of the poly-CoTAA film higher than the probing depth of the technique. XPS analysis of poly-CoTAA and Co(II)TPP used as a reference provides evidence of similarities between the two materials, in particular concerning the Co–N bonds(Fig. 2). The shape of the two Co(2p) spectra are very similar indicating the presence of a cobalt ion surrounded by four N atoms in both materials. The binding energies of the Co($2p_{3/2}$) and Co($2p_{1/2}$) peaks are equal to 781.1 and 796.4 eV, respectively. From these energy values and the shape of the O(1s) spectrum (Fig. S6. of ESI), the presence of metallic cobalt as well as cobalt oxides in the poly-CoTAA film are excluded.

The Co(2p) spectra for CoTPP and poly-CoTAA do not exhibit the expected multiplet structure associated to the Co(II) oxidation state (Fig. 2), in disagreement with the results on Co(II)TPP multilayers evaporated under vacuum.[50] We correlate this difference with the presence here of an unexpected O(1s) peak at about 532.5 eV (Fig. S6. of ESI), attributed to adsorbed water. This observation points to an effect of water molecules on the chemical environment of the cobalt ion. Hieringer et al.[50] have demonstrated that coordination of a NO ligand on the axial position of Co(II)TPP induces a shift of the binding energy peak towards high energy as well as the vanishing of the multiplet structure. This behavior is explained by a partial oxidation of the cobalt ion along with an increase of the electron density on the axial ligand. Following these results, we expect that water molecules also act here as a bound axial ligand, leading to the same conclusion and explaining fully our results. We note that the Co(2p) spectrum measured for a Co(II) diimine-dioxime complex

grafted on carbon nanotubes[28] is very close to those presented in Fig. 2. However, due to the absence of any significant shake-up satellites generally associated to Co(II), the authors have concluded that the oxidation level is Co(III) without further discussion. Because of the similarity with our work, bound axial ligand might well have modified the cobalt ion environment in that case too.

Two N(1s) spectra are presented in Fig. 2. For the Co(II)TPP reference, only one asymmetric peak is observed, in agreement with numerous studies reported in the literature.[51] The poly-CoTAA spectrum display a larger peak width explained by the appearance of new components in the high energy binding side of the peak. This change is correlated to the increase of an asymmetric tail of the C(1s) peak (Fig. S6 of ESI) indicating the presence of additional C≡N bonds in the poly-CoTAA film. Consequently, the N(1s)/Co(2p) ratio are different for the two compounds; i.e. 4/1 and 4.9/1 for CoTPP and poly-CoTAA respectively. We explain this result by the incorporation of nitrogen containing solvent (i.e. PhCN) inside the poly-CoTAA film during the electropolymerization process.

Kinetics of the HER at poly-CoTAA modified GC RDEs

Fig. 3 shows the voltammograms recorded at poly-CoTAA modified GC RDEs in N_2-purged 0.1 M NaCl buffered solutions. At pH 7.2, the voltammogram displays a large reduction wave at $E < -1.10$ V vs. SCE, but no plateau current. At pH 4.6, the onset of the reduction wave is positively shifted by ca. 160 mV, in good agreement with the shift of 0.156 mV predicted by the Nernst equation for an electrochemical reaction involving protons and electrons in a ratio 1 to 1; i.e. –60 mV pH^{-1}. Before direct reduction of water, a plateau current is reached between ca. –1.15 and –1.25 V vs. SCE. Control by the rate of mass transfer in this potential range is confirmed by the linear variation of the limiting current density i_L with the square root of the rotation rate ω (Fig. S7 of ESI), as expected from the Levich equation; i.e. $i_L = nB \times \omega^{1/2}$, where n is the number of electrons and B the so-called Levich constant. The limiting current density recorded at the poly-CoTAA modified RDE is comparable with that for H_2 evolution at a Pt RDE at the same rotation rate and in the same electrolyte (Fig. 3). Accordingly, the same number n of electrons (i.e. $n = 2$) is involved in the reduction process occurring

at the poly-CoTAA modified RDE. All these observations provide strong evidence that the electrochemical reaction occurring in acetate buffer is H_2 evolution in an overall two-electron reaction.

Since H_2 production consumes protons, measuring the increase of pH during electrolysis of an acidic solution provides an easy method to quantify the faradaic efficiency of a HER catalyst.[52] The charge passed during a 60 min electrolysis at –1.2 V vs. SCE of 2 mL of an acidified NaCl solution is 0.128 C (Fig. S8 of ESI), corresponding to a theoretical consumption of 6.63×10^{-4} M of H^+. In the meantime, the measured increase of 0.6 pH unit from pH 3.1 to pH 3.7 corresponds to an actual consumption of 5.95×10^{-4} M of H^+, establishing that poly-CoTAA operates at a faradaic efficiency of 90%.

The Tafel plot analysis of the voltammograms recorded at a poly-CoTAA modified RDE in acetate buffer solution indicates that the overpotential η varies linearly with the logarithm of the catalytic current density i_k over nearly two decades (Fig. S9 of ESI). The tafel slope $b = \partial\eta/\partial\log(-i_k)$ has a value of –122 mV dec^{-1} in the range $-0.32 > \eta > -0.47$ V. Extrapolation to zero overpotential gives an apparent exchange current density $i_0 = 2 \times 10^{-8}$ A cm^{-2}_{geom} (Table 1). Larger values of i_0 have been previously reported for electrodes grafted with Co diimine-dioxime and Co dithiolene.[28, 31] However, in these reports, the apparent exchange current density is calculated from Tafel plots exhibiting unusually high slopes (i.e. $\partial\eta/\partial\log(-i_k) >> -120$ mV dec^{-1}) and without taking into account the mass-transfer limitation.

The Tafel plots for the HER at poly-CoTAA in acetate buffer indicatethat an overpotential η = –0.57 V is required to reach a current density of –1 mA cm^{-2}_{geom}. This performance is comparable with that measured for an electrode grafted with Co diimine-dioxime.[28] On the other hand, electrode modified with Co dithiolene,[31] CoP_4N_2,[26] Co sulfide,[12] and Mo sulfide[8] exhibit larger catalytic performances (Table 1). From the surface concentration of Co sites in the poly-CoTAA film and the exchange current density, we can estimate here that the mass activity of Co at zero overpotential is i_0 ~ 0.09 A $(mg\ Co)^{-1}$. For comparison, Gasteiger and coworkers have found for the HER at Pt

nanoparticles a value of $i_0 \sim 0.35$ A (mg Pt)$^{-1}$ in 0.1 M KOH, and suggest that the mass activity of Pt is several orders of magnitude larger in 0.1 M $HClO_4$ than in 0.1 M KOH.[6]

The voltammograms recorded in the course of RDE measurements are stable (Fig. S7 of ESI), but the long-term stability of the poly-CoTAA film under strong H_2 evolution conditions also needs to be evaluated. Fig. 4 shows the current against time response recorded at an applied potential of –1.2 V vs. SCE in a 0.1 M NaCl solution buffered at pH 4.6. After a rapid decrease, the current density reaches a value of ca. –0.9 mA cm^{-2} that remains constant over a period of 30 min. But, when compared with the initial voltammogram, the voltammogram recorded after potentiostatic H_2 evolution during 30 min shows a negative shift by about 50 mV in the region of mixed control by mass transfer and activation, suggesting a decrease of the apparent concentration of Co sites. We ascribe this observation to partial demetallation of the poly-CoTAA film at negative potentials. The reduced stability upon H_2 evolution contrasts with the good stability previously observed upon O_2 reduction.[45] This result can however be understood considering the high reactivity of the reduced form of Co complexes with protons.

Mechanism of electrocatalytic H_2 evolution by poly-CoTAA

For a multistep electrochemical reaction, such as the HER, the Tafel slope can be used to establish the reaction mechanism from the value of the transfer coefficient $\alpha = \gamma/\nu + r\beta$,[53] where n is the total number of electrons, γ the number of electrochemical steps preceding the rate-determining step (rds), ν the number of time the rds occurs in the overall electrochemical reaction, r the number of electron exchanged in the rds, and β the charge transfer coefficient usually taken as 0.5. Here, the Tafel slope is $-2.3 \times RT/\alpha F \sim -120$ mV dec^{-1}, which gives $\alpha = 1/2$. With $n = 2$, we are left with two possibilities. First, $\gamma = 0$, $\nu = 1$ and $r = 1$, which corresponds to the following monomolecular pathway:

$$CoTAA + e^- + H^+ \rightarrow H\text{–}CoTAA \qquad (rds, \gamma = 0, \nu = 1, r = 1)$$

$$H\text{–}CoTAA + e^- + H^+ \leftrightarrows CoTAA + H_2 \qquad (fast)$$

Second, $\gamma = 1$, $\nu = 2$ and $r = 0$, which corresponds to the following bimolecular pathway:

234 $CoTAA + e^- + H^+ \leftrightarrows H{-}CoTAA$ (fast, $\gamma = 1$)

235 $2 \times H{-}CoTAA \rightarrow 2 \times CoTAA + H_2$ (rds, $\nu = 2$, $r = 0$)

236 Note that a monomolecular pathway, in which the second electrochemical step is the rds, would give
237 a Tafel slope of 40 mV dec^{-1}. Considering that the Co sites are immobilized on the electrode surface,
238 one might assume that the bimolecular pathway is here disfavored, but additional data collected
239 over a large pH range are required to obtain a more complete picture of the kinetics of the HER at
240 poly-CoTAA. Interestingly, both bimolecular and monomolecular pathways have been considered for
241 the catalysis of proton reduction by Co complexes in solution leading to mitigated conclusions.[4, 54-56].
242

243 ## Conclusions

244

245 Herein, we have shown that electropolymerization of CoTAA is a simple procedure to prepare a
246 cobalt-based molecular material electrocatalyzing H_2 evolution in acidic aqueous solution. Detailed
247 XPS analysis confirms that the structural integrity of the [Co^{II}–N_4] motif within the poly-CoTAA film is
248 preserved upon electropolymerization. RDE measurements in acetate buffer solution at pH 4.6 give a
249 catalytic current density $-i_k$ = 1 mA cm^{-2}_{geom} at an overpotential $\eta = -0.57$ V and an exchange current
250 density $i_0 \sim 0.09$ A (mg Co)$^{-1}$. A faradaic efficiency of 90% is achieved over a period of one hour of
251 electrolysis. The main limitation of poly-CoTAA as an electrocatalytic material for the HER is the
252 decrease of the surface concentration of the Co sites after prolonged H_2 evolution, we ascribe to
253 partial demetallation of the poly-CoTAA film at negative potentials. Finally, a Tafel slope value of
254 −120 mV dec^{-1} is consistent with a HER mechanism that follows either a monomolecular or a
255 bimolecular pathway. The latter is possibly disfavored considering that the Co sites are immobilized
256 on the electrode surface, but additional data are required to draw definitive conclusions
257

258 **Acknowledgments**

The kind assistance of J.-M. Kerboal for the synthesis of CoTAA is gratefully acknowledged. This work was supported by the Agence Nationale de la Recherche (ANR, BLANC SIMI9/0926-1, "TechBioPhyp"), the Centre National de la Recherche Scientifique (CNRS), and the Université de Bretagne Occidentale (UBO).

Electronic Supplementary Information

Additional XPS and electrochemical data are presented.

268

269 **References**

270 1. R. Parsons, *Trans. Faraday Soc.*, 1958, **54**, 1053-1063.

271 2. M. T. M. Koper and E. Bouwman, *Angew. Chem. Int. Ed.*, 2010, **49**, 3723-3725.

272 3. N. S. Lewis and D. G. Nocera, *Proc. Natl. Acad. Sci. U. S. A.*, 2006, **103**, 15729-15735.

273 4. J. L. Dempsey, B. S. Brunschwig, J. R. Winkler and H. B. Gray, *Acc. Chem. Res.*, 2009, **42**, 1995-
274 2004.

275 5. D. V. Esposito, S. T. Hunt, A. L. Stottlemyer, K. D. Dobson, B. E. McCandless, R. W. Birkmire
276 and J. G. Chen, *Angew. Chem. Int. Ed.*, 2010, **49**, 9859-9862.

277 6. W. Sheng, H. A. Gasteiger and Y. Shao-Horn, *J. Electrochem. Soc.*, 2010, **157**, B1529-B1536.

278 7. P. D. Tran and J. Barber, *PCCP*, 2012, **14**, 13772-13784.

279 8. T. F. Jaramillo, K. P. Jorgensen, J. Bonde, J. H. Nielsen, S. Horch and I. Chorkendorff, *Science*,
280 2007, **317**, 100-102.

281 9. D. Merki and X. Hu, *Energy Environ. Sci.*, 2011, **4**, 3878-3888.

282 10. A. B. Laursen, S. Kegnaes, S. Dahl and I. Chorkendorff, *Energy Environ. Sci.*, 2012, **5**, 5577-
283 5591.

284 11. H. I. Karunadasa, E. Montalvo, Y. Sun, M. Majda, J. R. Long and C. J. Chang, *Science*, 2012,
285 **335**, 698-702.

286 12. Y. Sun, C. Liu, D. C. Grauer, J. Yano, J. R. Long, P. Yang and C. J. Chang, *J. Am. Chem. Soc.*,
287 2013, **135**, 17699-17702.

288 13. M. Bourrez, R. Steinmetz, S. Ott, F. Gloaguen and L. Hammarstrom, *Nat. Chem.*, 2015, **7**, 140-
289 145.

290 14. M. L. Helm, M. P. Stewart, R. M. Bullock, M. R. DuBois and D. L. DuBois, *Science*, 2011, **333**,
291 863-866.

292 15. H. I. Karunadasa, C. J. Chang and J. R. Long, *Nature*, 2010, **464**, 1329-1333.

293 16. J. I. van der Vlugt, *Eur. J. Inorg. Chem.*, 2012, 363-375.

17. J. Willkomm, N. M. Muresan and E. Reisner, *Chem. Sci.*, 2015.
18. F. Gloaguen and T. B. Rauchfuss, *Chem. Soc. Rev.*, 2009, **38**, 100-108.
19. M. Rakowski Dubois and D. L. Dubois, *Acc. Chem. Res.*, 2009, **42**, 1974-1982.
20. M. Wang, L. Chen and L. Sun, *Energy Environ. Sci.*, 2012, **5**, 6763-6778.
21. V. S. Thoi, Y. Sun, J. R. Long and C. J. Chang, *Chem. Soc. Rev.*, 2013.
22. V. Artero, M. Chavarot-Kerlidou and M. Fontecave, *Angew. Chem. Int. Ed.*, 2011, **50**, 7238-7266.
23. Y. Sun, J. P. Bigi, N. A. Piro, M. L. Tang, J. R. Long and C. J. Chang, *J. Am. Chem. Soc.*, 2011, **133**, 9212-9215.
24. S. C. Marinescu, J. R. Winkler and H. B. Gray, *Proc. Natl. Acad. Sci. U. S. A.*, 2012, **109**, 15127-15131.
25. P. Zhang, M. Wang, F. Gloaguen, L. Chen, F. Quentel and L. Sun, *Chem. Commun.*, 2013.
26. L. Chen, M. Wang, K. Han, P. Zhang, F. Gloaguen and L. Sun, *Energy Environ. Sci.*, 2014, **7**, 329-334.
27. L. A. Berben and J. C. Peters, *Chem. Commun.*, 2010, **46**, 398-400.
28. E. S. Andreiadis, P.-A. Jacques, P. D. Tran, A. Leyris, M. Chavarot-Kerlidou, B. Jousselme, M. Matheron, J. Pecaut, S. Palacin, M. Fontecave and V. Artero, *Nat. Chem.*, 2012, **5**, 48-53.
29. A. Krawicz, J. Yang, E. Anzenberg, J. Yano, I. D. Sharp and G. F. Moore, *J. Am. Chem. Soc.*, 2013, **135**, 11861-11868.
30. O. Pantani, E. Anxolabehere-Mallart, A. Aukauloo and P. Millet, *Electrochem. Commun.*, 2007, **9**, 54-58.
31. A. J. Clough, J. W. Yoo, M. H. Mecklenburg and S. C. Marinescu, *J. Am. Chem. Soc.*, 2015, **137**, 118-121.
32. J. A. Widegren and R. G. Finke, *J. Mol. Catal. A: Chem.*, 2003, **198**, 317-341.
33. V. Artero and M. Fontecave, *Chem. Soc. Rev.*, 2013, **42**.

34. E. Anxolabehere-Mallart, C. Costentin, M. Fournier and M. Robert, *J. Phys. Chem. C*, 2014, **118**, 13377-13381.

35. B. D. McCarthy, C. L. Donley and J. L. Dempsey, *Chem. Sci.*, 2015.

36. K. M. Kadish, D. Schaeper, L. A. Bottomley, M. Tsutsui and R. L. Bobsein, *J. Inorg. Nucl. Chem.*, 1980, **42**, 469-474.

37. F. A. Cotton and J. Czuchajowska, *Polyhedron*, 1990, **9**, 2553-2566.

38. F. Beck, *J. Appl. Electrochem.*, 1977, **7**, 239-245.

39. C. L. Bailey, R. D. Bereman, D. P. Rillema and R. Nowak, *Inorg. Chem.*, 1986, **25**, 933-938.

40. C. L. Bailey, R. D. Bereman, D. P. Rillema and R. Nowak, *Inorg. Chim. Acta*, 1986, **116**, L45-L47.

41. P. J. Hochgesang and R. D. Bereman, *Inorg. Chim. Acta*, 1988, **149**, 69-76.

42. P. J. Hochgesang and R. D. Bereman, *Inorg. Chim. Acta*, 1990, **167**, 199-204.

43. A. Deronzier and M.-J. Marques, *Electrochim. Acta*, 1994, **39**, 1377-1383.

44. C. Miry, D. Le Brun, J.-M. Kerbaol and M. L'Her, *J. Electroanal. Chem.*, 2000, **494**, 53-59.

45. P. Convert, C. Coutanceau, P. Crouigneau, F. Gloaguen and C. Lamy, *J. Appl. Electrochem.*, 2001, **31**, 945-952.

46. J. R. Donat and K. W. Bruland, *Anal. Chem.*, 1988, **60**, 240-244.

47. M. Salou, B. Lescop, S. Rioual, A. Lebon, J. B. Youssef and B. Rouvellou, *Surf. Sci.*, 2008, **602**, 2901-2906.

48. A. Abelleira and F. Walsh, *Electrochim. Acta*, 1986, **31**, 113-117.

49. F. Gloaguen, F. Andolfatto, R. Durand and P. Ozil, *J. Appl. Electrochem.*, 1994, **24**, 863-869.

50. W. Hieringer, K. Flechtner, A. Kretschmann, K. Seufert, W. Auwarter, J. V. Barth, A. Gorling, H.-P. Steinruck and J. M. Gottfried, *J. Am. Chem. Soc.*, 2011, **133**, 6206-6222.

51. D. Karweik and N. Winograd, *Inorg. Chem.*, 1976, **15**, 2336-2342.

52. F. Quentel, G. Passard and F. Gloaguen, *Energy Environ. Sci.*, 2012, **5**, 7757-7761.

53. J. O. M. Bockris, A. K. N. Reddy and M. Gambao-Aldeco, *Modern Electrochemistry 2A: Fundamental of Electrodics*, Kluwer Academic/Plenum Publishers, New York, 2nd edn., 2001.

54. X. Hu, B. S. Brunschwig and J. C. Peters, *J. Am. Chem. Soc.*, 2007, **129**, 8988-8998.

55. C. Baffert, V. Artero and M. Fontecave, *Inorg. Chem.*, 2007, **46**, 1817-1824.

56. P. Du, J. Schneider, G. Luo, W. W. Brennessel and R. Eisenberg, *Inorg. Chem.*, 2009, **48**, 4952-4962.

57. T. F. Jaramillo, J. Bonde, J. Zhang, B.-L. Ooi, K. Andersson, J. Ulstrup and I. Chorkendorff, *J. Phys. Chem. C*, 2008, **112**, 17492-17498.

354

355 **Table 1**. Typical values of exchange current density i_0 and Tafel slope b reported in the literature for

356 the catalysis of the HER at chemically modified electrodes and inorganic materials.

Catalyst	**Loading** / **mol cm$^{-2}_{geom}$**	i_0 / **A cm$^{-2}_{geom}$**	b / **mV dec^{-1}**	**pH**	**Ref**
CoTAA	1.4×10^{-8}	2×10^{-8}	122	4.6	this work
Co-diimine-dioxime	4.5×10^{-9}	3.2×10^{-7}	160[(a)]	4.5	[28]
Co-dithiolene	3.7×10^{-6}	5.0×10^{-6}	> 150[(a)]	4.2	[31]
$[Mo_3S_4]^{4+}$	1.6×10^{-11}	2.2×10^{-7}	120	0.4	[57]
Co sulfide	–	2.6×10^{-4}	93	7.0	[12]
Mo sulfide	–	3.1×10^{-7}	55–60	0.2	[8]

357 [(a)]Tafel plot calculated without correction of the voltammogram for the mass transfer limitation in

358 solution

359

360

361 **Figures**

362

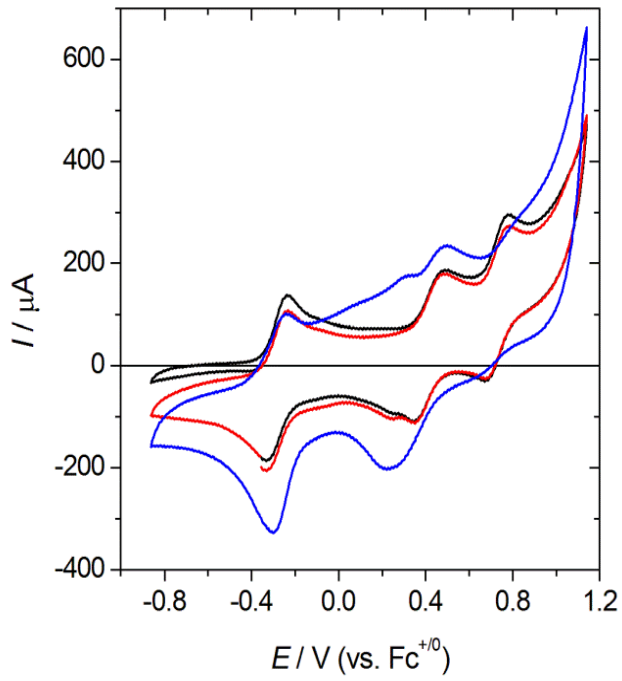

363

364 **Fig. 1.** Voltammograms recorded upon continuous potential scanning at 0.1 V s^{-1} at a gold-coated

365 glass slide electrode of ca 1 cm^2 in surface area immersed in a solution of about 2 mM CoTAA in 0.1

366 M Bu_4NPF_6/PhCN: 1st scan (black trace), 2nd scan (red trace) and 30th scan (blue trace).

367

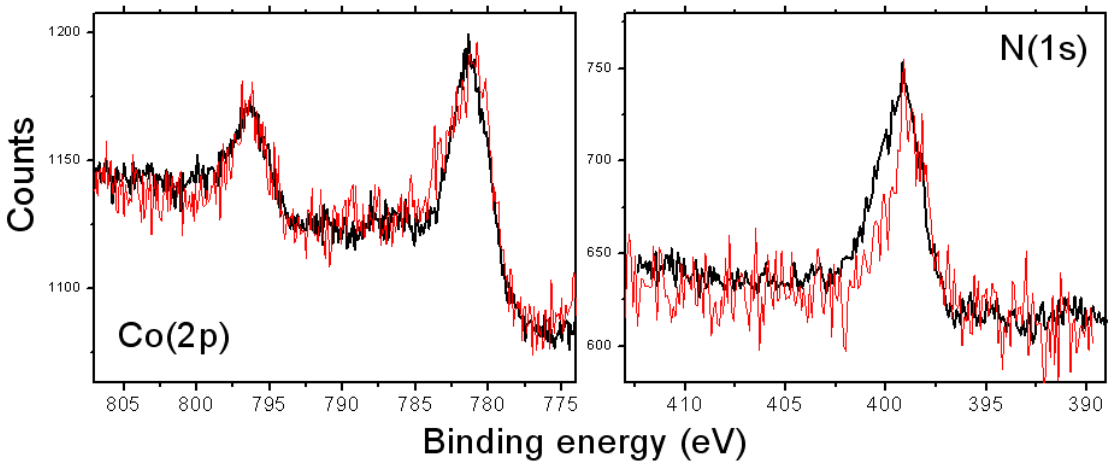

Fig. 2. XPS signals of a poly-CoTAA film (black trace) and of Co(II)TPP (red trace) used as a reference compound.

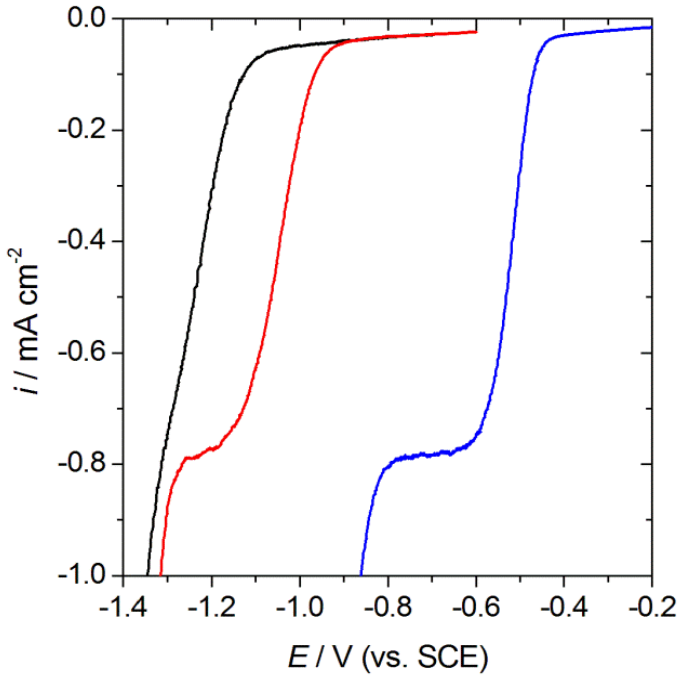

Fig. 3. Voltammograms recorded at 5 mV s^{-1} and 500 rpm at a poly-CoTAA modified RDE in 0.1 M NaCl and 6 mM PBS (pH 7.2, black trace) and in 0.1 M NaCl and 6 mM acetate buffer (pH 4.6, red trace). The response of a Pt RDE in 0.1 M NaCl and 6 mM acetate buffer is also shown (blue trace).

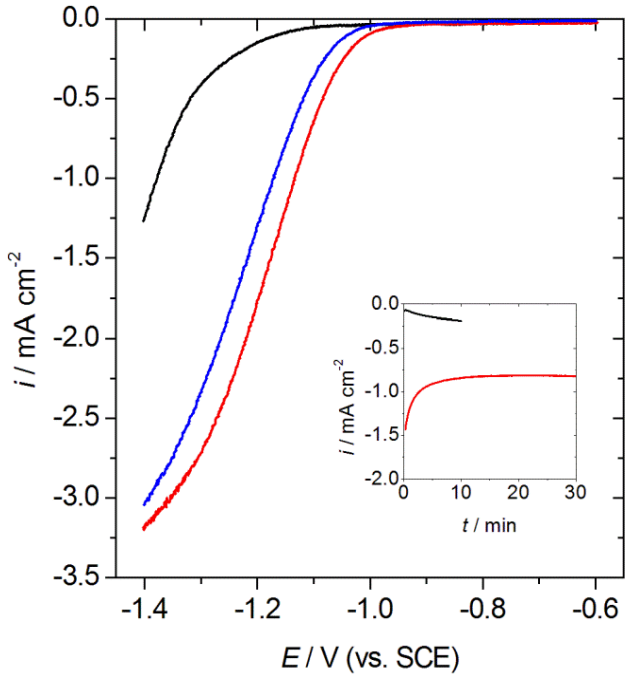

Fig. 4. Voltammograms recorded at 5 mV s^{-1} and 500 rpm in 0.1 M NaCl and 17 mM acetate buffer (pH 4.6) at a bare GC electrode (black trace) and a poly-CoTAA modified electrode before (red trace) and after (blue trace) prolonged H_2 evolution. The inset shows the current density against time plots recorded at a potential of −1.2 V vs. SCE and 200 rpm at a bare GC electrode (black trace) and a poly-CoTAA modified electrode (red trace).

Table of contents entry

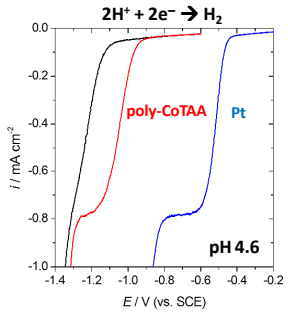

Electropolymerization of CoTAA gives electrocatalytic material for the H_2 evolution reaction in acidic aqueous solution